ISSN: 2577 - 8005

Clinical Case Report

Medical & Clinical Research

Effective radiotherapy in rarely observed para-aortic lymph node metastases of sinonasal schwannoma-clinical case from our practice

Lena Marinova*, Vaska Vasileva, Iliya Gabrovski, Nikolai Kahchiev, Radoslav Radev

[1]*Department of Radiation Oncology and Metabolic Brachytherapy, Medical Oncology Clinic, UMHAT "Queen Joanna" Sofia, Bulgaria.*

***Corresponding Author**
Lena Marinova, Department of Radiation Oncology and Metabolic Brachytherapy, Medical Oncology Clinic, UMHAT "Queen Joanna" Sofia, Bulgaria.

Submitted: 03 Jun 2023; **Accepted**: 12 Jun 2023; **Published**: 20 Jun 2023

Citation: *Marinova L, Vasileva V, Gabrovski I, Kahchiev N, Radev R (2023) Effective radiotherapy in rarely observed para-aortic lymph node metastases of sinonasal schwannoma-clinical case from our practice. Medical & Clinical Research 8(6), 01-11.*

Abstract

Schwannoma is benign neurogenic tumor, that arise from Schwann cells of the peripheral nerve sheath. Malignant schwannomas transformation is extremely rare. Histopathological and immunohistochemical analysis confirmed the final pathohistological diagnosis, which is extremely important for the assessment of the therapeutic approach. Schwannomas lymph node metastases are extremely rare and poorly characterized. We present an extremely rare sinonasal schwannoma with metastases in the para-aortic lymph nodes. More interesting is that metastatic para-aortic lymph nodes were affected by radiotherapy .

In this article, we share the surprising fact, that the proved through FDG-PET/CT para -aortic lymph node metastases in sinonasal schwannoma with a limitation of more than 3 years, is effectively responded after radiotherapy with total dose over 45 Gy.

Keywords: Sinonasal Schwannoma, Histopathological Analysis, Immunohistochemical Analysis, Para-Aortic Lymph Node Metastases, Fdg-Pet/Ct, Radiotherapy

Introduction

Schwannoma is a benign, encapsulated, slow-growing and generally solitary tumour that arise from Schwann cells of the peripheral nerve sheath [1-4]. This tumor was first described by Verocay in 1910, who coined the term "neurilemmoma" to describe this benign neurogenic tumor [5]. Schwannoma can be found at any age, although most commonly found between the 3rd and 6th decades, and it has no gender preference [6]. Schwannomas are the most common type of peripheral nerve tumors, but their incidence is low and comprises one per 50,000 individuals [7]. Extracranial schwannomas in the head and neck region comprise 25-45% of all schwannomas, but only 4% involve the nasal cavity and paranasal sinuses [3,8-10]. Schwannoma is generally a benign tumour, but there are a few cases showing malignant transformation reported in the literature [11,12]. There are several reports [13-15] of schwannomas misdiagnosed as lymph nodes metastasis or malignant tumors detected by FDG-PET [16]. We present an extremely rare malignancy of sinonasal schwannoma with lymphatic metastases in the para-aortic lymph nodes.

Clinical Case

We present a 60-year-old woman. At the end of 2020, there were complaints of a headache, a progressive one-sided nasal obstruction, a gradually reduced left-wing vision and exophthalmus of the left eye.

MRI/March 2021: The brain substance of T2-FLAIR and other sequences are with isointense signal without changes in the brain ventricles. The pituitary gland has a preserved structure and sizes. Rightly, a 14 mm/6 mm soft tissue formation is visualized, destroying adjacent bones, engaging the sphenoid sinus and ethmoid sinuses bilateral, entering the two nasal passages, more in the right, and infiltrating the left retrobulbar space (Figure 1A,B,C). March 2021 an endonasal biopsy with a histological result an inflammatory myofibroblastic tumor was performed. From the immunohistochemical (IHC) examination- spindle cells express Vimentin, do not expose ALK 1; About 10% of plasmocytes expose the IG G4. Due to the diagnosis of a slow growing border tumor, the patient is evaluated for active monitoring. In April 2021, the patient suffered an endoscopic medial orbital decompression to the left.

Local Status: A pronounced exophthalmus on the left eye. Hyperemic and leaked nasal mucosa, without possible nasal cavity inspection. Non palpable enlarged cervical lymph nodes bilaterally.

Intraoperative: After the opening of the left maxillary sinus, an anterior and posterior ethmoidectomy was performed, as a large part of the ethmoid cells were destroyed and infiltrated by the tumor. The tumor originates from the right sphenoid sinus, destroying the adjacent bones and engaging bilateral ethmoid cells, enters the two nasal vestibules, more to the right and extends to the left retro-

bulbar space. It reached the anterior wall of the sphenoid sinus, whose bone is infiltrated by the tumor. The sphenoid sinus opened and cleaned from the tumor to the rhinobase. Moderate bleeding was manifested, and after stopping it moved to endoscopic medial decompression of the orbit of the left eye. The lamina papyracea was removed and an incision of periorbital tissue was performed. Sent material for histological examination from the anterior wall of the left sphenoid sinus and from the left periorbital tumor tissue.

Consultation of the Histological Result: The material represents bone fragments and tumor proliferation with the following characteristics: 1/Biphasic cell proliferation;2/Spindle cell schwannoma (fascicular scar) and vacuolized areas; 3/ The cells have unclearly distinguished cytoplasm, dense chromatin, without axons; 4/No mitotic figures are observed; 5/Degenerative changes/hyalinization (Figures 2A,B,C and Figure 3).

From Immunohistochemical (IHC) Analysis: Tumor cells with positive expression to the S100 Protein and to the Vimentin (Figure 4A,B). Figure 5/A presents the tumor cells negative to CK AE1/AE3; Negative expression to Desmin and to Myogenin (Figure 5B,C). Only the walls of blood vessels and scattered cells in the Antoni B zones are positive to CD 34 (Figure 5D). Based on pathohistological and immunohistochemical analysis, this tumor was defined as sinonasal schwannoma. After non-radical surgery, the patient is evaluated for active monitoring. Given the benign disease nature and its slow growth, the patient is not directed for radiotherapy (RT). After a year of partial surgery, complaints of headaches and secretions from the nasal cavity are restored, and the vision of the left eye with exophthalm completely disappears. MRI January 2022 visualizes a soft tissue tumor engaging the sphenoid sinus and ethmoidal sinuses bilateral, which destroys the adjacent bones and enters the two nasal passages and infiltrates the left retrobulbar space (Figure 6). Due to the available symptoms, it was estimated to carry out intensity modulated radiotherapy (IMRT) in the tumor area with a daily dose (DD) 2 Gy up to total dose (TD) 66 Gy (Figure 7). The patient has suffered RT without radiation reactions. After 3 months, a control MRI was conducted to establish tumor stationation, lack of visible reduction or progression (Figure 8). 6 months after the end of radiotherapy (RT), the patient is in good general condition, without symptoms and of good quality of life. It is subject to active monitoring. After 9 months of the RT completion, a FDG-PET/CT was carried out, which reported para-aortic lymph metastases at the level of Th 12-L2.

From PET/CT November 2022: Retroperitoneal to the right ventral of L2 is visualized a soft tissue formation up to 30 mm, probably a conglomerate paracaval lymph nodes with high metabolic activity SUV Max 5.2 and with secondary nature. A similar soft tissue finding with a diameter of 21mm with high metabolic activity SUV Max 5.7 settles left between Th 12 and L1 (Figure 9). IMRT in the area of para-aortic lymph nodes from Th 10-L3 with daily dose (DD) 3 Gy up to total dose (TD) 30 Gy was carried out with simultaneous boost in metastases with DD 3.5 Gy up to TD 35 Gy (Figures 10,11 and 12). From PET/CT (May 2023) after 6 months of the RT completion, no metabolic activity in the para-aortic and para-caval lymph nodes were established (Figure 13).

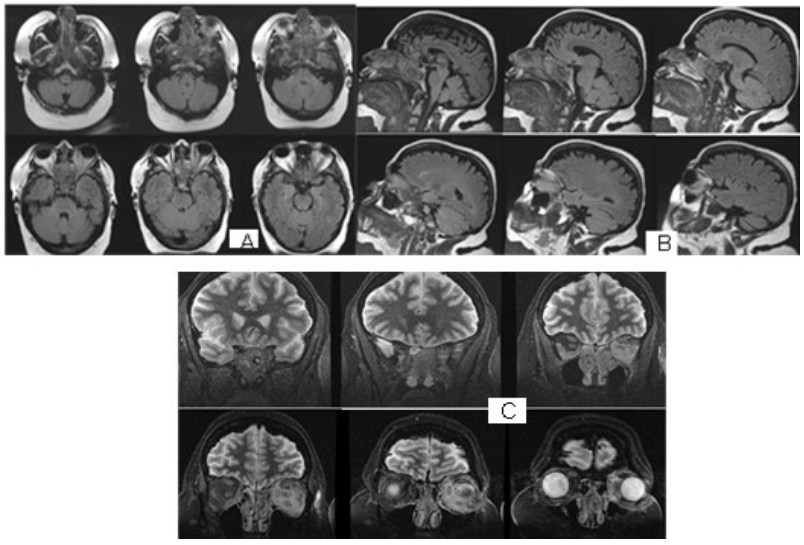

Figure 1: A/B) Axial and sagittal MRI/March 2021-The brain substance of T2-FLAIR and other sequences are with isointense signal without changes in the brain ventricles. Rightly, a 14 mm/6 mm soft-tissue formation is visualized, destroying adjacent bones, engaging the sphenoid sinus and ethmoid sinuses bilateral, entering the two nasal passages, more in the right, and infiltrating the left retrobulbar space;C) Coronal MRI.

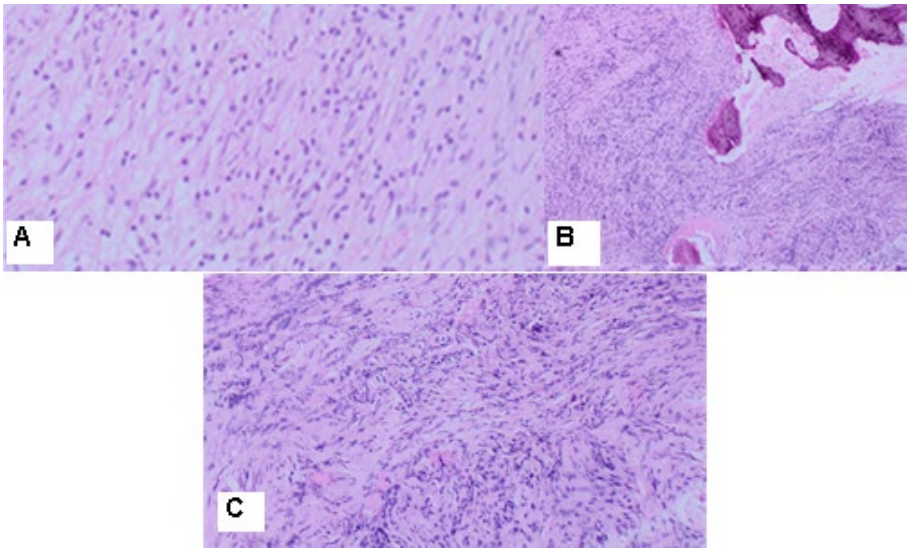

Figure 2: Microscopic histological findings. A) Tumor cells have ill defined cytoplasm and dense chromatin pattern H&Ex40; B) Spindle cells show interlacing pattern and palisading of nuclei with expressed hyalinization of tumor stroma; Bone structures are visualized at the top right, and below to the right whorling pattern H&Ex 20; C) Areas with many cells and a small amount of cells; Spindle cells show interlacing pattern and palisading of nuclei; whorling pattern on the right; expressed hyalinization of tumor stroma.H&Ex100.

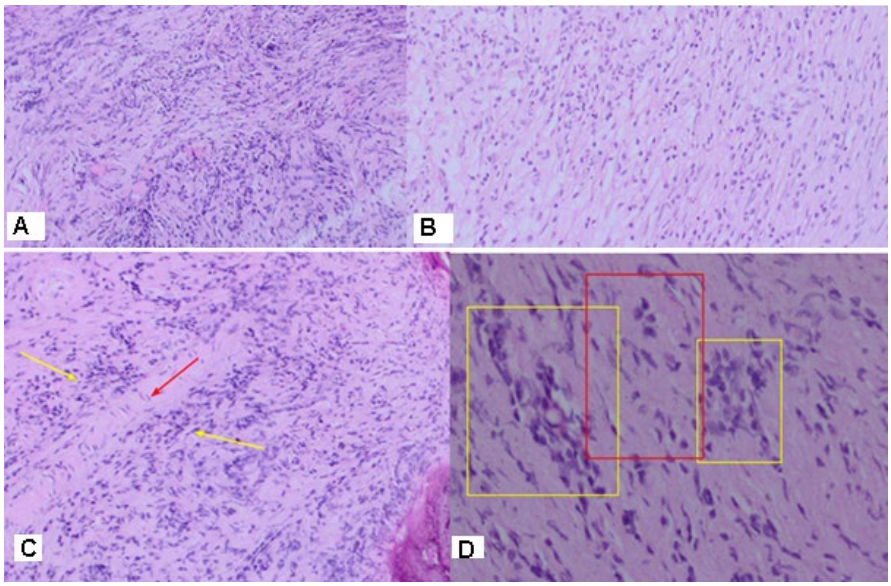

Figure 3: Microscopic histological findings. A) Spindle cells show interlacing pattern and palisading of nuclei; whorling pattern on the right H&Ex20; B) Cells are narrow, elongated and wavy with tapered ends interspersed with collagen fibers H&Ex20; C) At high power (H&Ex40) the palisading nuclei and Verocay bodies are evident, as well as the Antony A and Antony B components (the yellow arrows show Antony A and Antony B components, and the red arrow shows parallel arrays of nuclei forming a Verocay body); D) At high power (H&Ex100) the palisading nuclei and Verocay bodies are evident, as well as the Antony A and Antony B components (the yellow rectangles show Antony A and Antony B components, and the red shows parallel arrays of nuclei forming a Verocay body).

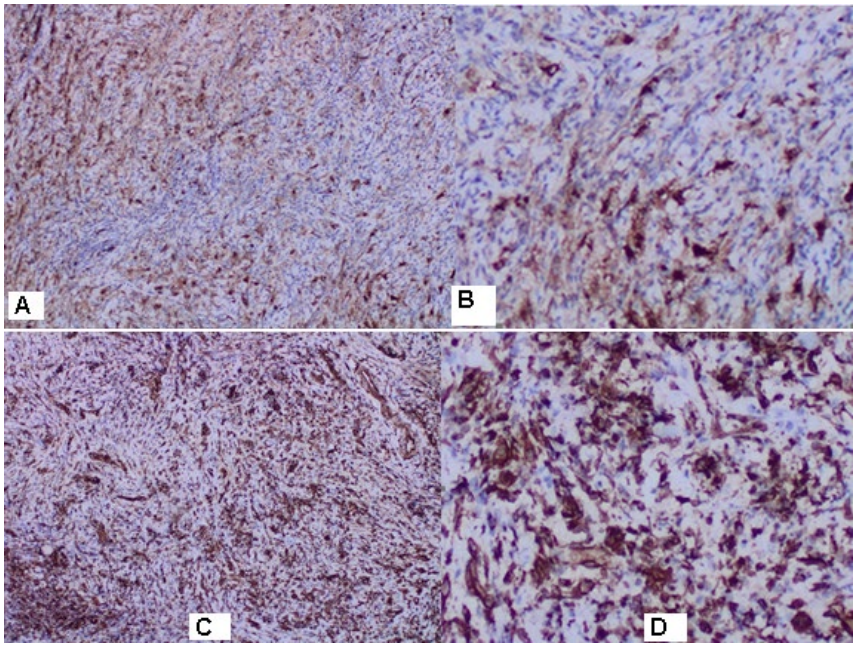

Figure 4: Immunohistochemistry. A/B) Tumor cells with positive expression to S100 protein (at low power H&Ex100 and at high power H&Ex400); C/D) Tumor cells with positive Vimentin expression (at low power H&Ex100 and at high power H&Ex400).

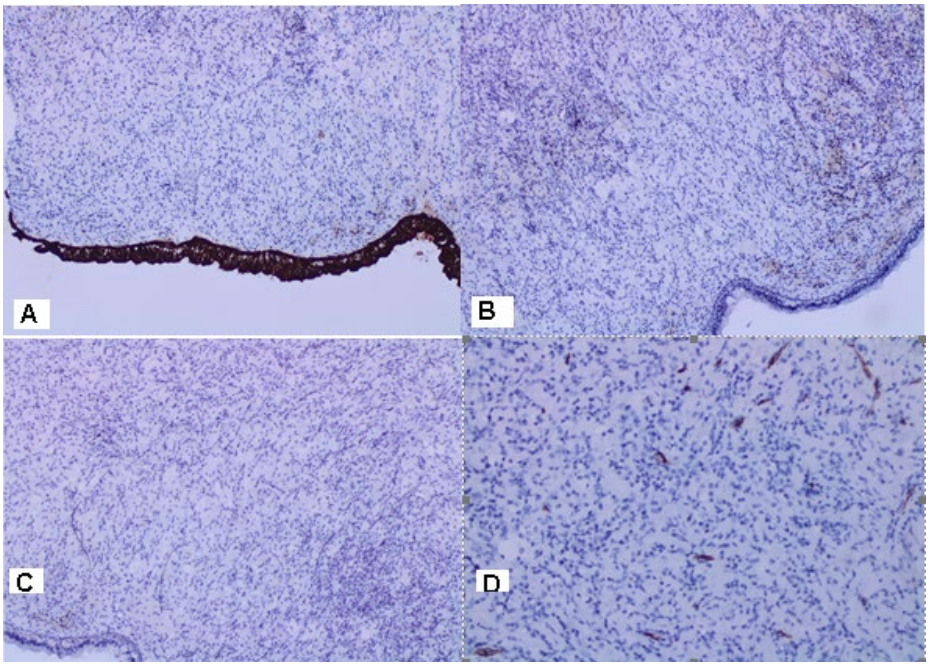

Figure 5: Immunohistochemistry. A) Tumor cells with negative CK AE1/AE3 expression; B) Negative expression to Desmin; C) Negative expression to Myogenin; D) Only the walls of the blood vessels and scattered cells in Antoni B areas are marked to the CD 34.

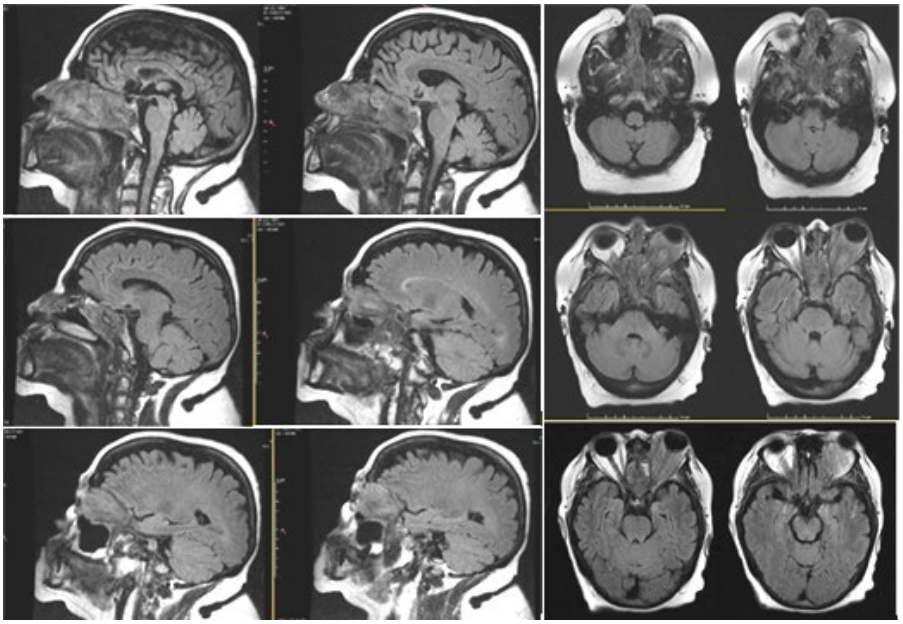

Figure 6: MRI/January 2022-Sag T2 FLAIR and AxT2 FLAIR visualizes a soft tissue tumor engaging bilateral the sphenoid sinus and ethmoidal sinuses, which destroys the adjacent bones and enters the two nasal passages and infiltrates the left retrobulbar space.

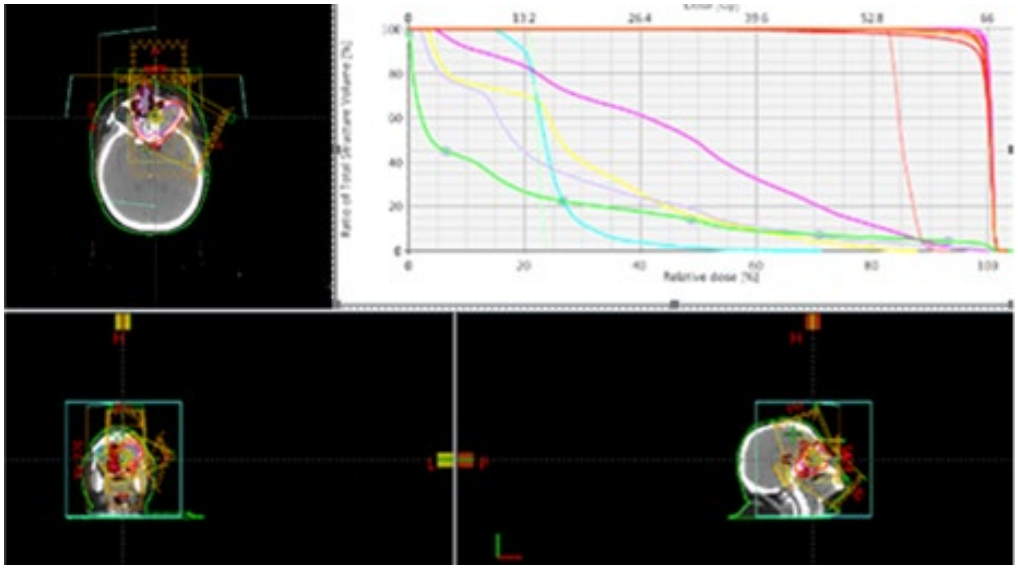

Figure 7: Intensity modulated radiotherapy (IMRT) by the VMAT method in the primary sinonasal tumor with a daily dose 2 Gy up to total dose 66 Gy.

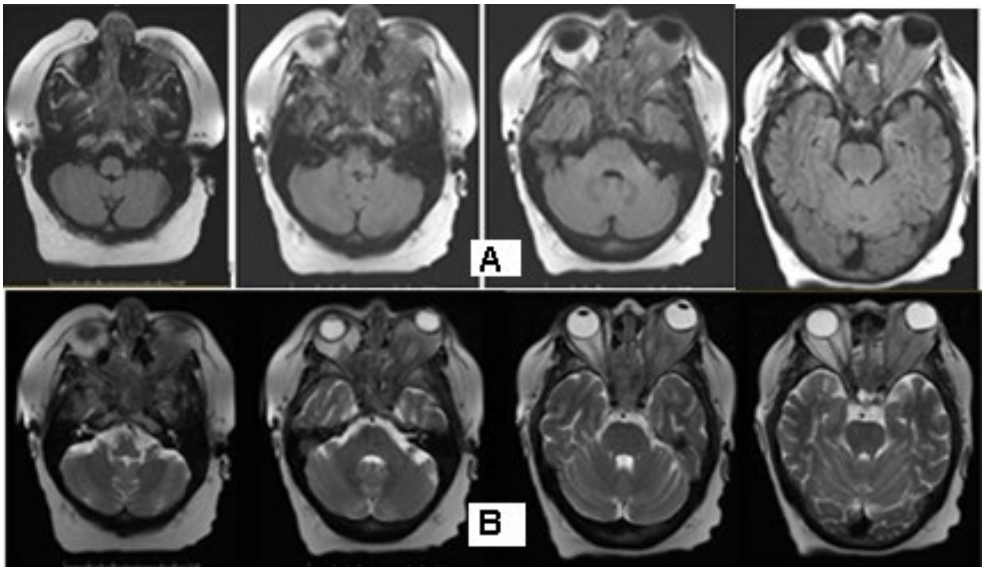

Figure 8: Axial MRI 3 months after the radiotherapy completion represent a tumor stationation without reduction or progression-A/ AxT2 FLAIR B/AxT2 FRFSE.

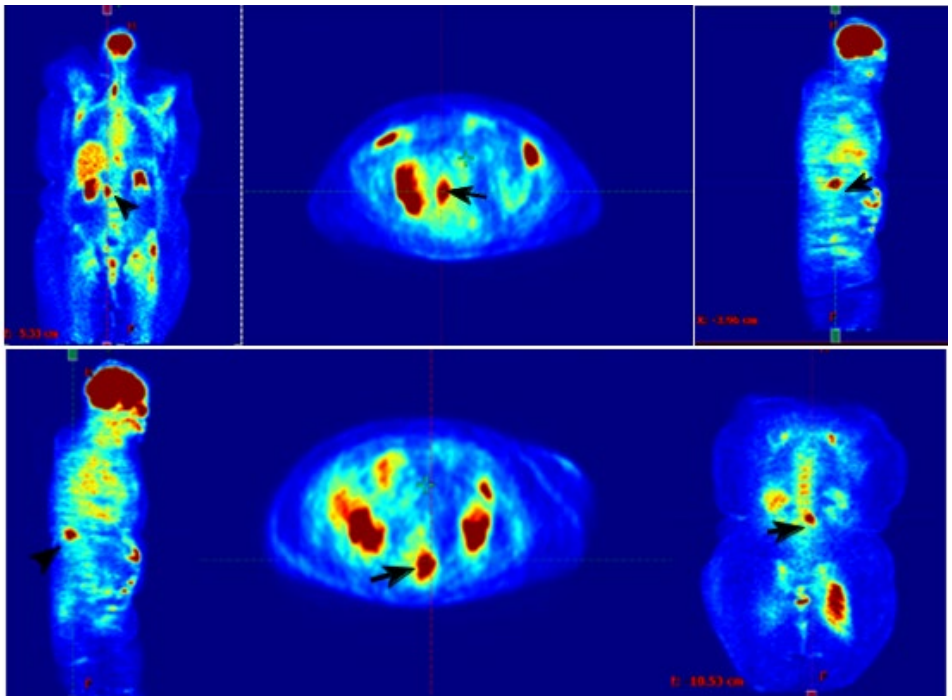

Figure 9: PET/CT-Para-aortic lymph node metastases on level Th 12-L2 (shown with black arrows).

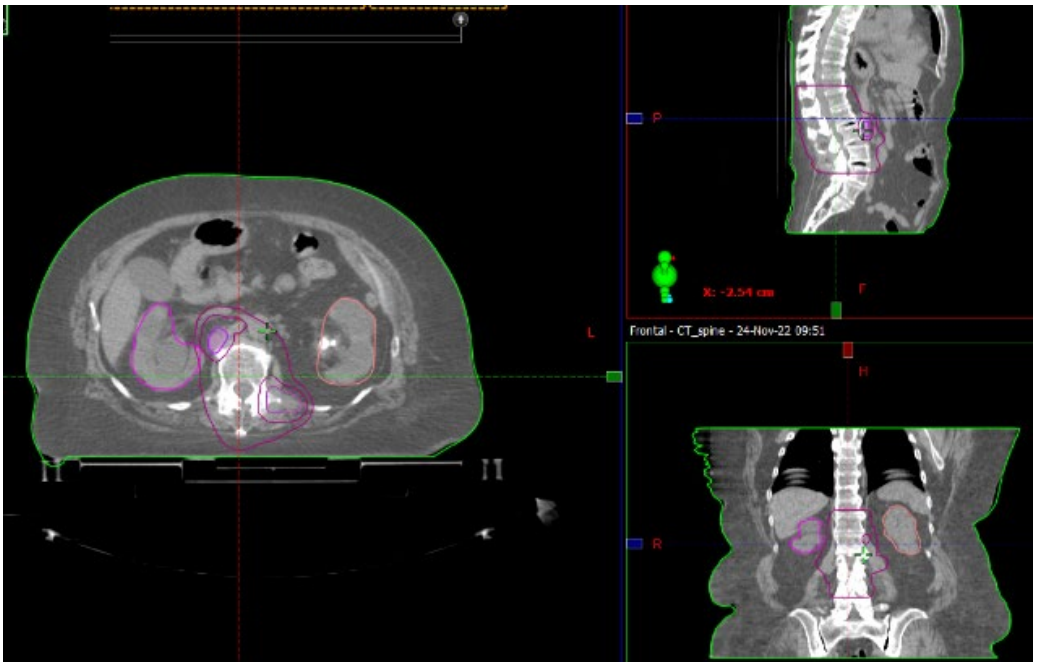

Figure 10: Radiotherapy planning-CT with conturing of the clinical target volumes and the normal surrounding organs and structures.

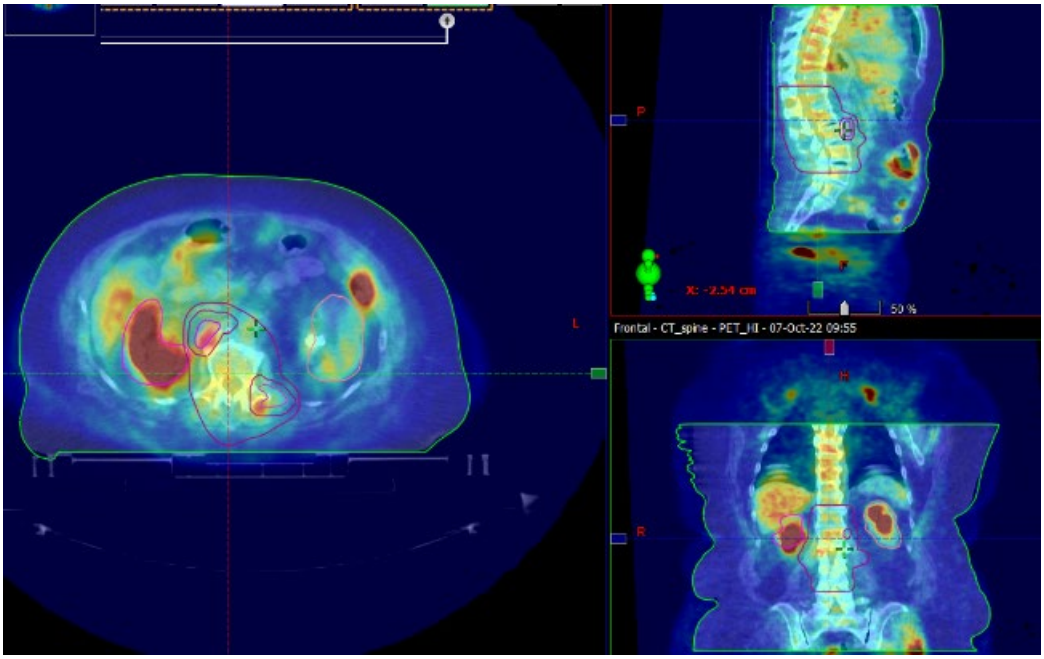

Figure 11: Radiotherapy planning Fusion of CT with PET/CT, where you can see very well metabolically active para-aortic lymph node metastases. In this way, the targeted volumes in which the therapeutic radiation dose should be realized are determined.

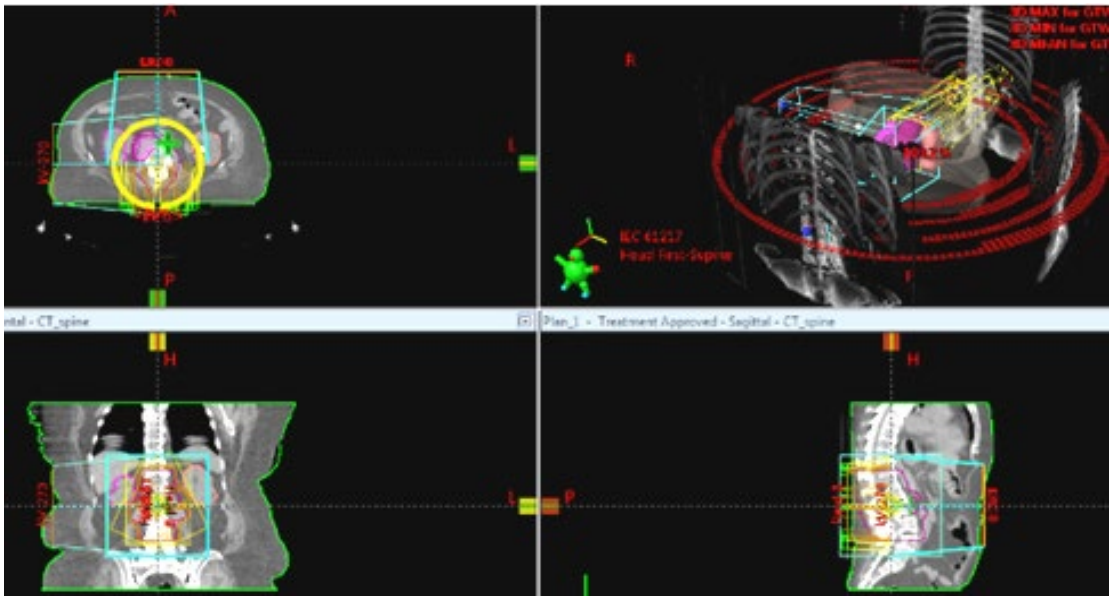

Figure 12: IMRT in the area of para-aortic lymph nodes from Th 10-L3 with daily dose (DD) 3 Gy up to total dose (TD) 30 Gy with simultaneous boost in metastases with DD 3.5 Gy up to TD 35 Gy

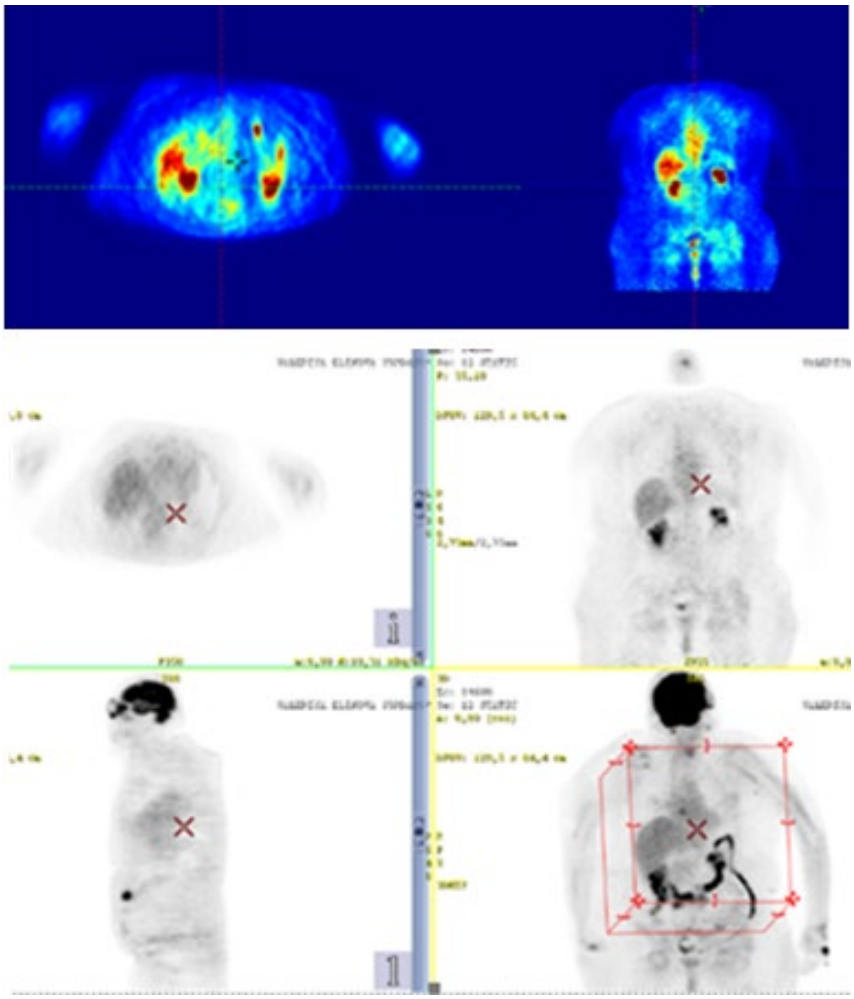

Figure 13: PET/CT/May 2023 after 6 months of the RT completion without metabolic activity in the para-aortic lymph nodes

Discussion

The schwannomas can emerge from any nerve covered with a Schwann cell sheath, including the cranial nerves (with the exception of the optic and olfactory nerves), the spinal nerves, and the autonomous nervous system [17]. Retroperitoneal schwannomas are extremely rare, comprising only 1% of all schwannomas [18]. In sinonasal cavity, schwannomas are postulated to arise from the ophthalmic and maxillary branches of the trigeminal nerve or from autonomic nerves to the septal vessels and mucosa [19]. The ethmoid sinus is the most common site of sinonasal location, followed by the maxillary sinus, the nasal cavity and the sphenoid sinus [20].

Sinonasal region, even though it is located in the head, has an extremely low incidence (about 4%) of Schwannomas [10,21]. They have a variety of morphological appearances, but they behave as World Health Organization (WHO) grade I tumors [2]. Malignant transformation within a schwannoma usually results in an epithelioid or primitive neuroectodermal morphology [22,23]. Pre-operative diagnosis is difficult and further investigations are needed such as MRI, CT, US and angiography [24]. The typical features on MRI are a well-circumscribed small nodule, homogeneously isointense to muscle on T1WI and homogeneously hyperintense on T2WI, showing homogeneous enhancement after contrast administration [25]. In the presented clinical case, MR T2 FLAIR images of the tumor are isointense to muscle tissue (Figure 1A,B,C). Histopathological and immunohistochemical (IHC) analyses confirmed the diagnosis [1]. The histopathological material represents tumor proliferation with the following characteristics: 1/biphasic cell proliferation (cellular Antoni A & hypocellular Antoni B); 2/ Spindel schwannoma cell (fascicular scar) and vacuolized areas; 3/ The cells with unclearly distinguished cytoplasm, dense chromatin, axons generally absent within lesion; 4/ No mitotic figures are observed; 5/Degenerative changes/hyalinization (Figures 2 and 3). The histological diagnosis of schwannoma is usually apparent because of the presence of alternating patterns of Antoni A and B areas, nuclear palisading, Verocay bodies, and the whirling of cells, histological finding that we present in Figure 3C,D. Schwannomas are characterized by strong and diffuse immunoreactivity for S-100 protein, which is the clue for the diagnosis [26-28]. The presence of S-100 protein in IHC staining is a classic marker for diagnostic confirmation and magnetic resonance imaging (MRI) is the gold standard for preoperative imaging [29]. There is some truth to the contention that schwannomas express S100 to a greater extent than neurofibromas, but because of a degree of overlap in the expression of this marker between these two tumors, relying on this stain alone is not sufficient [30]. In our clinical case, we report a positive expression of tumor cells to S100 protein and Vimentin (Figure 4). Figure 5A represents tumor cells with negative CK AE1/AE3 expression and a well visible spinocellular epithelium; negative expression to Desmin and to Myogenin (Figure 5B,C). As schwannomas are typically benign, well circumscribed, and minimally invasive tumors, complete surgical excision is the standard of care for ensuring no recurrence [31-35]. The surgical techniques used varied according to time, before the year 2000 the surgeries were performed using an external approach or a combination of an external and endonasal approach [36]. In our clinical case, intraoperatively observed destroying the adjact bones, which is also visible to MRI.It is not completely clear whether this bone lysis is due to a malignant transformation or is the result of a slow tumor growth, leading to erosion of adjacent bone structures. Hayasaka et al. reported that benign schwannoma on MR showed low signal intensities on T1-weighted images and high signal intensities on T2-weighted images, in contrast with malignant schwannoma which exhibit mixed-signals and are composed of solid and hemorrhagic cystic components on both T1-and T2-weighted images. However, the authors also mentioned that primary retroperitoneal schwannoma have no specific characteristics [37]. Patients require active monitoring with PET/ CT as schwannomas generally show high FDG uptake [38-40]. It is well known that the schwannomas have a characteristic dual pattern with areas that are highly (Antony A) and less (Antony B) cellular, and the degree of cellularity varies widely among lesions; therefore, these tumors can display a wide range of SUVs (0.33-3.7 and 1.9-7.21, respectively) [41,42].

These tumours do not respond to radiotherapy [43]. In our clinical case, it is a locally advanced sinonasal schwannoma originating in the sphenoid sinus and the engagement of the clivus, which defines the inoperable tumor. After decompressive surgery, the tumor continued to grow slowly and the symptoms involving headaches were manifested again (Figure 6). After a year, the symptoms intensified, which necessitated decompressive RT. Due to the benign nature of the disease, we have judged a high radical total radiation dose to reduce the tumor volume and stop the tumor growth. Due to the tumor radioresistance, we conducted IMRT up to a high total dose (TD) 66 Gy (Figure 7). After 3 months, MRI reported a tumor of the same size, without reduction or progression (Figure 8). After 9 months of the RT completion, the 18F-Fluorodeoxyglucose (FDG) Positron Emiision Tomography (PET) has reported increased metabolic activity of the tumor (SUV Max 9.2), which has proven the exceptional radioresistance of primary sinonasal schwannomas. Surprisingly, para-aortic lymph node metastases at the level of Th 12- L2 with increased metabolic activity SUV Max 5.2-5.7 were detected (Figure 9), which proves the rare possibility of malignant transformation, that requires prolonged monitoring of patients with shwannomas [44,45]. PET/CT criterion for a positive SUVmax is greater than 2.5 [16]. Schwannomas lymphatic node metastases are extremely rare and poorly characterized in the literature [46,47].Intranodal schwannomas are rare and only a few reports have been described in the English literature (<15 cases) [12,16,48). In most of these reports, schwannomas were located in retroperitoneal or pericolic lymph nodes [49-51]. Despite the pronounced radioresistance of the primary tumor, we conducted the IMRT in the field of para-aortic lymph nodes from the level of Th 10-L3 with DD 3 Gy up to TD 30 Gy with simultaneous boost in para-aortic lymph node metastases with DD 3.5 Gy up to TD 35 Gy /BED 47.25 Gy (Figures 10, Figure 11, Figure 12). PET/CT from May 2023 reported lack of metabolic activity in the field of para-aortic lymph node metastases (Figure 13). In English literature this is the only clinical case of primary sinonasal scwannoma with metastases by lymphatic pathway in para-aortic lymph nodes. More interesting is that metastatic para-aortic lymph nodes were affected by RT.

Conclusion

Inoperable schwannoma is a benign, encapsulated, slow-growing and generally solitary tumour that arise from Schwann cells of the peripheral nerve sheath. Histopathological and immunohistochemical examination confirmed the diagnosis. If possible, the basic treatment involves radical surgery. The primary inoperable schwannoma is extremely radioresistance, despite the realization of a high radiation dose that has a symptomatic effect. Prolonged monitoring of patients is required as tumor malignance with distant lymph node metastases are possible. Since it is well known that tumor metastases are less differentiated than the primary tumor, the palliative RT up to TD above 45 Gy, achieves local control of inoperable lymph node metastases.

References

1. Abreu I, Roriz D, Rodrigues P, Moreira Â, Marques C (2017) Schwannoma of the tongue-A common tumour in a rare location: A case report. Eur J Radiol Open 4:1-3.
2. Hilton DA, Hanemann CO (2014) Schwannomas and their pathogenesis. Brain Pathol 24:205-220.
3. Swain SK, Samal S, Das S, Padhy R (2021) A Large Intraoral Sublingual Schwannoma in a Pediatric Patient: A Case Report. Iran J Otorhinolaryngol 33(118):335-337.
4. Rajiv J (2012) Learning from eponyms: Jose Verocay and Verocay bodies, Antoni A and B areas, Nils Antoni and Schwannomas. Indian Dermatol Online J (3):215-219.
5. Lollar WK, Pollak N, Liess DB (2010) Schwannoma of the hard palate. Am J Otolaryngol 31(2):139-140.
6. Kavcic J, Bozic M (2016) Schwannoma of the tongue. BMJ Case Rep 1-4.
7. Hanemann CO, Evans DG (2006) News on the genetics, epidemiology, medical care and translational research of Schwannomas. J Neurol 253:1533-1541.
8. Berlucchi M, Piazza C, Blanzuoli L, Battaglia G, Nicolai P (2000) Schwannoma of the nasal septum: a case report with review of the literature. Eur Arch Otorhinolaryngol 257:402-405.
9. A El-Saggan, J Olofsson, B Krossnes (2003) Sinonasal schwannoma: two case reports and review of literature. Int Congress Series 1240:503-507.
10. Buob D, Wacrenier A, Chevalier D, Aubert S, Quinchon JF, et al. (2003) Schwannoma of the sinonasal tract: a clinicopathologic and immunohistochemical study of 5 cases. Archives of Pathology and Laboratory Medicine 127 (9):1196-1199.
11. Kindblom LG, Ahldén M, Meis-Kindblom JM, Stenman G (1995) Immunohistochemical and molecular analysis of p53, MDM2, proliferating cell nuclear antigen and Ki67 in benign and malignant peripheral nerve sheath tumors. Virchows Arch 427(1):19-26.
12. Silvestre CF, Tavares JA, López-Presa D, Dos Santos VR, Rocha J,et al. (2019) Cervical Lymph Node Schwannoma-An Unexpected Diagnosis Clin Pathol 12:2632010X19829239.
13. Ortega-Candil A, Rodríguez-Rey C, Cabrera-Martín MN, García García-Esquinas M, Lapeña-Gutiérrez L, et al. (2013) 18FDG PET/CT imaging of schwannoma mimicking colorectal cancer metastasis. Rev Esp Med Nucl Imagen Mol 32(5):332-333.
14. Fujii T, Yajima R, Morita H, Yamaguchi S, Tsutsumi S, et al. (2014) FDG-PET/CT of schwannomas arising in the brachial plexus mimicking lymph node metastasis: report of two cases. World J Surg Oncol 12:309.
15. Igai H, Kamiyoshihara M, Kawatani N, Ibe T, Shimizu K (2014) Sternal intraosseous schwannoma mimicking breast cancer metastasis. J.Cardiothorac Surg 27(9):116.
16. Kamiyoshihara M, Igai H, Ohsawa F, Yoshikawa R, Yazawa T, et al. (2018). Schwannoma arising in a lymph node mimicking metastatic pulmonary carcinoma. Respir Med Case Rep 25:18-21.
17. Harada H, Omura K, Maeda A (2001) A massive pleomorphic adenoma of the submandibular salivary gland accompanied by neurilemomas of the neck misdiagnosed as a malignant tumor: report of case. J Oral and Maxillofacial Surgery 59(8):931-935.
18. Das Gupta TK, Brasfield RD, Strong EW, Hajdu SI (1969) Benign solitary Schwannomas (neurilemomas). Cancer 24:355-366.
19. Hegazy HM, Snyderman CH, Fan CY, Kassam AB (2001) Neurilemmomas of the paranasal sinuses. Am J Otolaryngol 22:215-218.
20. 20. Sheikh HY, Chakravarthy RP, Slevin NJ, Sykes AJ, Banerjee SS, et al. (2008) Benign schwannoma in paranasal sinuses: A clinicopathologicalstudy of five cases, emphasising diagnostic difficulties. J Laryngol Otol 122: 598-602.
21. Hillstrom RP, Zarbo RJ, Jacobs JR (1990) Nerve sheath tumors of the paranasal sinuses: electron microscopy and histopathologic diagnosis. Otolaryngol Head and Neck Surgery 102(3):257-263.
22. McMenamin ME, Fletcher CD (2001) Expanding the spectrum of malignant change in schwannomas: epithelioid malignant change, epithelioid malignant peripheral nerve sheath tumor, and epithelioid angiosarcoma: a study of 17 cases. Am J Surg Pathol 25:13-25.
23. Woodruff JM, Selig AM, Crowley K, Allen PW (1994) Schwannoma (neurilemoma) with malignant transformation. A rare, distinctive peripheral nerve tumor. Am J Surg Pathol 18:882-895
24. C Bocciolini, S Cavazza, P Laudadio (2005) Schwannoma of cervical sympathetic chain: assessment and management.Acta Otorhinolaryngol Ital 25(3):191-194.
25. Cohen M, Wang B (2009) Schwannoma of the tongue: two case reports and review of the literature. Eur Arch Otorhinolaryngol 266:1823-1829.
26. Fisher C (2011) 2nd edition. Amirsys; Diagnostic Pathology: Soft Tissue Tumors.
27. Lindberg MR (2016) 2nd edition. Amirsys; Diagnostic Pathology: Soft Tissue Tumors.
28. Weiss SW, Nickoloff BJ (1993) CD-34 is expressed by a distinctive cell population in peripheral nerve, nerve sheath tumors, and related lesions. Am J Surg Pathol 17:1039-1045.
29. Singh GB, Arora R, Garg S, Aggarwal K (2015) Base of tongue schwannoma. ENT-Ear, Nose & Throat J 306-308.
30. Rodney T. Miller (2004) Immunohistochemistry in the Differ-

ential Diagnosis of Schwannoma and Neurofibroma Immunohistochemistry Newsletter.
31. Mehrzad H, Persaud R, Papadimitriou N, Kaniyur S, Mochloulis G, et al. (2006) Schwannoma of tongue base treated with transoral carbon dioxide laser. Lasers Med Sci 21(04):235-237.
32. Rathore AS, Srivastava D, Narwal N, Shetty DC (2015) Neurilemmoma of Retromolar Region in the oral cavity. Case Rep Dent 2015:320830.
33. Biswas D, Marnane CN, Mal R, Baldwin D (2007) Extracranial head and neck schwannomas-a 10-year review. Auris Nasus Larynx 34:353-359.
34. Melvin WS, Wilkinson MG (1993) Gastric schwannoma. Clinical and pathologic considerations. Am Surg 59:293-296.
35. Pasquini E, Sciarretta V, Farneti G, Ippolito A, Mazzatenta D, et al. (2002) Endoscopic endonasal approach for the treatment of benign schwannoma of the sinonasal tract and pterygopalatine fossa. Am J Rhino 16:113-118.
36. Riveros AC, Proietti V, Serrano C, Ruggerics (2021) Sinonadal Schwannomas. J Otolaryngol Rhinol 7:108.
37. Hayasaka K, Tanaka Y, Soeda S, Huppert P, Claussen CD (1999) MR findings in primary retroperitoneal schwannoma. Acta Radiol 40:78-82.
38. Ohno T, Ogata K, Kogure N, Ando H, Aihara R, et al. (2011) Gastric schwannomas show an obviously increased fluorodeoxyglucose uptake in positron emission tomography: report of two cases. Surg Today 41:1133-1137.
39. Ahmed AR, Watanabe H, Aoki J, Shinozaki T, Takagishi K (2001) Schwannoma of the extremities: the role of PET in preoperative planning. Eur J Nucl Med 28:1541-1551.
40. Beaulieu S, Rubin B, Djang D, Conrad E, Turcotte E,, et al. (2004) Conrad E, Turcotte E, Eary JF: Positron emission tomography of schwannomas: emphasizing its potential in preoperative planning. AJR Am J Roentgenol 182:971-974.
41. Beaulieu S, Rubin B, Djang D, Conrad E, Turcotte E, et al. (2004) Positron emission tomography of schwannomas: emphasizing its potential in preoperative planning. AJR Am J Roentgenol 182:971-974.
42. Benz MR, Czernin J, Dry SM, Tap WD, Allen-Auerbach MS, et al. (2010) Quantitative F18-fluorodeoxyglucose positron emission tomography accurately characterizes peripheral nerve sheath tumors as malignant or benign. Cancer 116:451-458.
43. Sutay S, Tekinsoy B, Ceryan K, Aksu Y (1993) Submaxillary hypoglossal neuri-lemmoma. J Laryngol Otol 107:953-954.
44. Kandasamy S, Nathan RS, John RR (2017) Neurilemmoma of maxillary alveolus: a rare case report and review of literature. J Pharm Bioallied Sci 9(1):285-288.
45. Sethi D, Sethi A, Nigam S, Agarwal A (2008) Schwannoma of oral tongue: a rare benign neoplasm. The International Journal of Head and Neck Surgery 3(1):84-96.
46. Medina-Gallardo A, Curbelo-Peña Y, Molinero-Polo J, Saladich-Cubero M, De Castro-Gutierrez X, et al. (2017) Saladich-Cubero M, De Castro Gutierrez X, Vallverdú-Cartie H. Mesenteric intranodal schwannoma: uncommon case ofneurogenic benign tumor. J Surg Case Rep 2:1-2.
47. Black JO, Zhai QJ, Varona OB, Ordonez NG, Luna MA. (2010) Primary schwannoma in a cervical lymph node. Head Neck 32:964-969.
48. Piana S, Gelli MC, Cavazza A, Serra L, Gardini G (2002) Ancient schwannoma arising in a lymph node: report of a case and review of literature. Pathol Res Pract 198(1):51-54.
49. Nam K, Namkung S (2011) Intranodal schwannoma mimicking a gastrointestinal stromal tumor of the stomach: a case report. J Korean Soc Radiol 65:395-398.
50. Ji J, Yoo J, Kang SJ, Lee KY (2009) Schwannoma arising in a lymph node-a brief case report. Korean J Pathol 43:271-273.
51. Nasrin S, Shahriar S (2008) Schwannoma in a perigastric lymph node: a rare case report. Iran J Pathol 1:43-46.

Copyright: *©2023 Lena Marinova, et al. This is an open-access article distributed under the terms of the Creative Commons Attribution License, which permits unrestricted use, distribution, and reproduction in any medium, provided the original authors and source are credited.*